© 2023 Hefei Institutes of Physical Science, Chinese Academy of Sciences and IOP Publishing Printed in China and the UK

Plasma Sci. Technol. **25** (2023) 085504 (9pp) https://doi.org/10.1088/2058-6272/acc14c

Dielectric barrier discharge plasma synthesis of Ag/γ-Al_2O_3 catalysts for catalytic oxidation of CO

Yunming TAO (陶云明)[1], **Yuebing XU** (胥月兵)[1], **Kuan CHANG** (常宽)[1], **Meiling CHEN** (陈美玲)[1], **Sergey A STAROSTIN**[2], **Hujun XU** (许虎君)[1] and **Liangliang LIN** (林良良)[1,*]

[1] Key Laboratory of Synthetic and Biological Colloids, Ministry of Education, School of Chemical and Material Engineering, Jiangnan University, Wuxi 214122, People's Republic of China
[2] FUJIFILM Manufacturing Europe, Tilburg Research Labs, Tilburg 5047 TK, Netherlands

E-mail: linliangliang@jiangnan.edu.cn

Received 18 December 2022, revised 28 February 2023
Accepted for publication 3 March 2023
Published 19 April 2023

Abstract

In this study, Ag/γ-Al_2O_3 catalysts were synthesized by an Ar dielectric barrier discharge plasma using silver nitrate as the Ag source and γ-alumina (γ-Al_2O_3) as the support. It is revealed that plasma can reduce silver ions to generate crystalline silver nanoparticles (AgNPs) of good dispersion and uniformity on the alumina surface, leading to the formation of Ag/γ-Al_2O_3 catalysts in a green manner without traditional chemical reductants. Ag/γ-Al_2O_3 exhibited good catalytic activity and stability in CO oxidation reactions, and the activity increased with increase in the Ag content. For catalysts with more than 2 wt% Ag, 100% CO conversion can be achieved at 300 °C. The catalytic activity of the Ag/γ-Al_2O_3 catalysts is also closely related to the size of the γ-alumina, where Ag/nano-γ-Al_2O_3 catalysts demonstrate better performance than Ag/micro-γ-Al_2O_3 catalysts with the same Ag content. In addition, the catalytic properties of plasma-generated Ag/nano-γ-Al_2O_3 (Ag/γ-Al_2O_3-P) catalysts were compared with those of Ag/nano-γ-Al_2O_3 catalysts prepared by the traditional calcination approach (Ag/γ-Al_2O_3-C), with the plasma-generated samples demonstrating better overall performance. This simple, rapid and green plasma process is considered to be applicable for the synthesis of diverse noble metal-based catalysts.

Supplementary material for this article is available online

Keywords: DBD plasma, plasma nanofabrication, noble metal nanoparticles, CO oxidation, Ag/γ-Al_2O_3 catalysts

(Some figures may appear in colour only in the online journal)

1. Introduction

Catalysts, by reducing the activation energy or changing the reaction mechanism, are essential in the chemical industry for their ability to accelerate reactions, reducing costs and giving increased conversion efficiency and product selectivity. It is well recognized that 85%–90% of industrial chemical processes, including the production of commodity chemicals, petrochemicals, pharmaceuticals and fine chemicals, involve at least one catalytic step [1]. The application of catalysts not only opens up the possibility of using renewable, safe or more readily available materials, but also allows simplification of operating conditions in terms of pressure and temperature [2]. Thus, catalysis has induced rapid development of the modern chemical industry.

In most cases, metals are considered to be at the core of the performance of catalysts. Among these, noble metal-based catalysts have attracted great attention due to their superior

* Author to whom any correspondence should be addressed.

catalytic activity and durability. In past decades, much effort has been directed towards the design and synthesis of noble metal catalysts. Despite substantial progress, especially in the synthesis of catalysts with high activity and stability, several issues remain to be addressed. Traditional preparation methods such as precipitation/co-precipitation [3], calcination [4], sol–gel [5], flow chemistry [6, 7], chemical deposition [8], etc typically entail a series of steps, requiring tedious and time-consuming pre-/post-treatments such as washing, drying, calcination, reduction in hydrogen gas and activation. Meanwhile, such methods often need large volumes of solvents, which inevitably bring contaminants (Cl^-, SO_4^{2-}, NO_3^-, etc) and pollutants to the catalysts as well as the environment. Apart from that, high-temperature calcination together with a long reaction time would boost particle growth and aggregation, leading to the deterioration of catalytic activity.

To meet the ever-increasing demand for 'greener' processes, it would be highly desirable to develop new approaches for the preparation of catalysts with a simplified process, shorter reaction times and reduced solvent consumption. In recent years, plasma has been actively explored as an efficient way to synthesize nanomaterials such as carbon dots [9], silver nanoparticles (AgNPs) [10], AuNPs [11, 12], Ag–Au alloys [13], etc. Due to the presence of diverse reactive species (electrons, ions, excited atoms, molecules), plasma can stimulate reactions and achieve processes under milder conditions [14–16]. A dielectric barrier discharge (DBD) is a non-equilibrium cold plasma that can be operated at atmospheric pressure with different gases. Compared with other plasma types, it is more adaptable to conventional processes and complex devices. The low-heating nature and capacity for long-term stable operation further makes DBD a green and energy-saving approach for preparing nanomaterials [17]. When applied in catalyst production, DBD plasma demonstrates benefits such as reduced particle size, improved dispersion, enhanced metal–support interactions and increased catalytic activity [18, 19]. As a result, various catalysts have been prepared by the DBD plasma method, including CeO_2 [20], MnO_x/γ-Al_2O_3 [21] and Ni/BN [22].

Carbon monoxide (CO) is a toxic gas that may cause severe damage to the human body and the environment, and requires proper conversion to avoid direct release into the environment. Some important chemical industrial processes such as methanol re-forming often generate CO as an intermediate which may inhibit the target reaction by blocking the active sites of catalysts, leading to catalyst poisoning. As a consequence, production yields are significantly reduced [23]. In addition, CO oxidation, as one of the typical reactions of heterogeneous catalysis, is commonly used as a model case reaction for understanding the catalytic mechanism [24, 25]. Therefore, catalytic CO oxidation is of great significance both for academic research and practical application. On the other hand, it should be noted that CO oxidation may lead to CO_2 emission and the greenhouse effect, but the negative impacts are much less than those of CO (e.g. catalyst poisoning, environmental or human threats). Different strategies have been developed for CO_2 capture and storage, making CO oxidation an effective way to reduce the undesired effects of CO.

In the present work, γ-alumina-supported silver catalysts (Ag/γ-Al_2O_3) were prepared using a DBD plasma setup, with the aiming of finding an efficient green method to produce noble metal-based catalysts without complex steps, organic solvents and H_2 reduction. In particular, silver-based catalysts exhibit good prospects for CO oxidation, and alumina as the catalyst support offers the advantages of Lewis acidity and basicity, good porosity and resistance to high temperatures. Compared with traditional preparation methods, an important highlight of this study is the elimination of the H_2 reduction setup. This avoids serious the hazards of operating with hydrogen plasma at atmospheric pressure and makes the approach more suitable for practical applications. The effects of the Ag content and the size effect of the Al_2O_3 support on the catalytic performance were evaluated through the CO oxidation reaction and compared with Ag/γ-Al_2O_3 catalysts prepared by the traditional calcination method (Ag/γ-Al_2O_3-C).

2. Experiment

2.1. Preparation of the Ag/γ-Al$_2$O$_3$ catalysts

In this study, an atmospheric pressure DBD plasma setup was employed for the synthesis of the Ag/γ-Al_2O_3 catalysts, as shown in figure 1(a). For comparison, we also prepared Ag/γ-Al_2O_3 catalysts using the standard calcination method following the procedure described in a previous study [26]; these are denoted as Ag/γ-Al_2O_3-C for simplification. Unless mentioned otherwise, Ag/nano-γ-Al_2O_3 catalysts refer to the catalysts prepared by the DBD plasma method using nano-sized γ-Al_2O_3 as the support, while Ag/micro-γ-Al_2O_3 catalysts refer to the catalysts obtained by the plasma method using a microsized γ-Al_2O_3 support. As for the DBD plasma setup, two stainless steel (SS) disks functioned as the electrodes and were connected to an AC high-voltage power supply (CTP-2000 K, Nanjing Suman Electronics Co. Ltd, China) and grounded, respectively. A quartz DBD reactor consisting of a sample cell (diameter 62 mm, height 8 mm) and a dish (diameter 96 mm, thickness 2 mm) was inserted between the electrodes. Upon the supply of high-voltage power to the electrodes, plasma discharges were formed within the DBD reactor (figure S1). An Ar flow was coupled into the reactor as the working gas, the flow rate of which could be regulated by a mass flow controller (MFC, Bronkhorst High-Tech B.V.).

The catalyst preparation process is schematically shown in figure 1(b). In a typical procedure, an appropriate amount of γ-Al_2O_3 was added to silver nitrate solution under stirring to obtain the catalyst precursors with different Ag loadings (0.5 wt%, 1 wt%, 2 wt%, 4 wt%, 8 wt%); these were then dried at 70 °C for 1 h to obtain solid powder. After grinding, 0.5 g of the powder was transferred and uniformly placed in the DBD reactor for plasma treatment. In the plasma media, Ar ions, electrons and atomic excited states are produced via

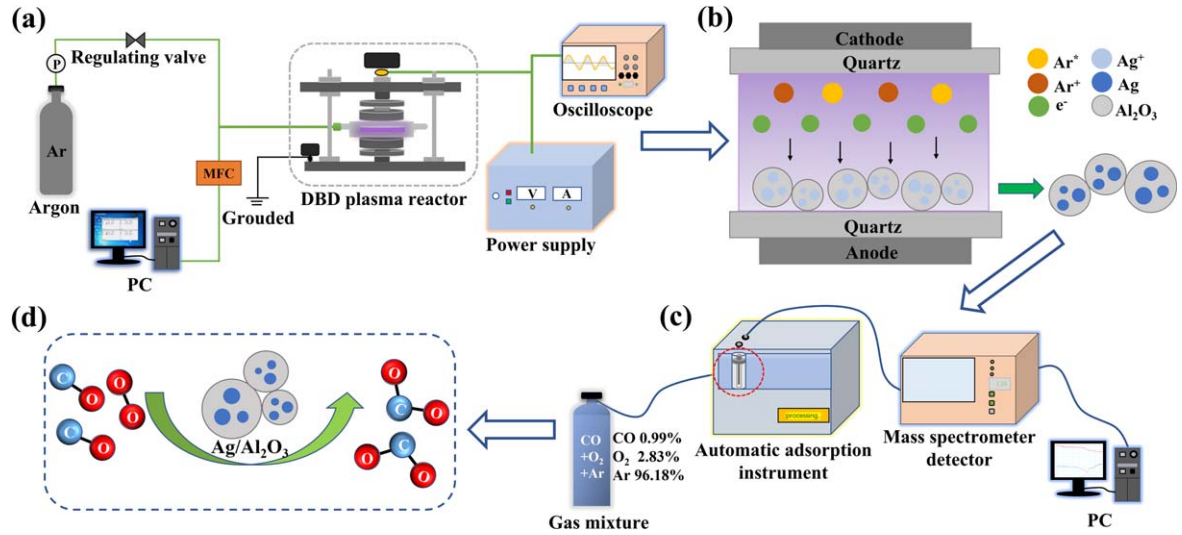

Figure 1. (a) Schematic diagram of the DBD plasma setup for the preparation of $Ag/\gamma\text{-}Al_2O_3$ catalysts. (b) Illustration of the catalyst preparation process. (c) The automatic chemical adsorption apparatus for evaluation of the catalysts. (d) Schematic of CO oxidation on the $Ag/\gamma\text{-}Al_2O_3$ catalysts.

various ionization and excitation processes. While the detailed Ag reduction mechanism requires further investigation, we speculated that the electrons coming from the plasma to the surface can reduce the silver ions loaded on the alumina to form AgNPs. At the same time, the excited species originating in the plasma may also contribute to the reduction of silver ions. The Ar flow rate and plasma exposure time were fixed at 30 ml min^{-1} and 10 min, respectively, to ensure maximum constancy in all experiments. After the plasma treatment, the samples were removed from the DBD reactor for further characterization. The charge (Q) and voltage (V) waveforms during experiments were recorded using a Tektronix-TBS1102 digital oscilloscope and utilized to calculate the dissipated energy in the discharge with a Lissajous curve.

2.2. Characterization of Ag/γ-Al$_2$O$_3$ catalysts

The radiative excited species in the plasma were characterized by an ER4000-EX optical emission spectrometer (OES; Shanghai Chen Chang Inc.). The morphology of the catalysts was examined with a S-4800 scanning electron microscope (SEM; Hitachi, Ltd, Japan), with a silicon drift energy dispersive x-ray spectrometer (EDX) to analyze the element information. The shape and size of the catalysts were characterized by a JEM-2100plus transmission electron microscope (TEM; Hitachi, Ltd, Japan) operated at an accelerating voltage of 200 kV. The surface chemical composition and binding information were further studied with a Kratos Axis Supra x-ray photoelectron spectrometer (XPS; Shimadzu Kratos, Japan). The crystal structure of the catalysts was determined by x-ray diffraction (XRD) on a Bruker AXS GmbH diffractometer using Cu Kα radiation (Kα = 1.54056 Å). Diffuse reflectance UV–visible spectra (DRUV) were recorded on a UV-3600 plus spectrophotometer (Hitachi, Ltd, Japan) at room temperature in air, with $BaSO_4$ as the reference.

2.3. Evaluation of the catalytic performance of Ag/γ-Al$_2$O$_3$

The catalytic performance of the $Ag/\gamma\text{-}Al_2O_3$ catalysts was evaluated by means of the temperature programmed surface reaction (TPSR) using an automatic chemical adsorption apparatus (BELCAT-II, MicrotracBEL Corporation, Japan), as shown in figure 1(c). Typically, 100 mg of the $Ag/\gamma\text{-}Al_2O_3$ catalysts was placed in the quartz reactor of the apparatus and flushed with Ar for 10 min at 50 °C. A precisely prepared $CO/O_2/Ar$ (with $CO/O_2/Ar$ 0.99/2.83/96.18% v/v) mixture with a 30 ml min^{-1} flow rate was introduced into the system as the reaction gas. Then, the system was heated up to 700 °C at a ramping rate of 10 °C min^{-1}, during which the CO oxidation reaction on the $Ag/\gamma\text{-}Al_2O_3$ catalysts (figure 1(d)) was investigated by analyzing the gas composition using an online mass spectrometer. The CO conversion efficiency was calculated using the following formula [27]:

$$\text{CO conversion} = \frac{[\text{CO}]_{\text{in}} - [\text{CO}]_{\text{out}}}{[\text{CO}]_{\text{in}}} \times 100\%$$

where $[CO]_{in}$ and $[CO]_{out}$ respectively represent the concentration of the CO before and after reaction at a certain temperature.

3. Experimental results

3.1. DBD plasma synthesis of Ag/γ-Al$_2$O$_3$ catalysts

The discharge characteristics of the DBD plasma were first studied to obtain a general overview of the synthesis process. Figure 2(a) shows a typical V–Q diagram during the experiments. Periodic sinusoidal voltage waveforms with a peak-to-peak value of 20.6 kV were observed. The plasma power is calculated to be 3.12 W from the corresponding Lissajous curve (figure 2(b)). A representative emission spectrum

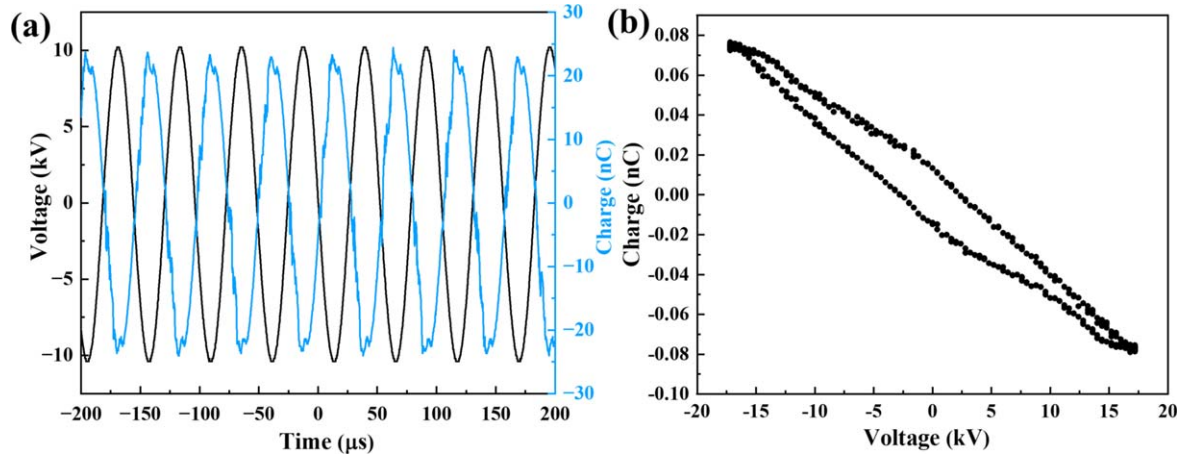

Figure 2. (a) *V*–*Q* diagram recorded during the plasma preparation of Ag/nano-γ-Al_2O_3. (b) The corresponding Lissajous curve for calculation of the dissipated plasma power.

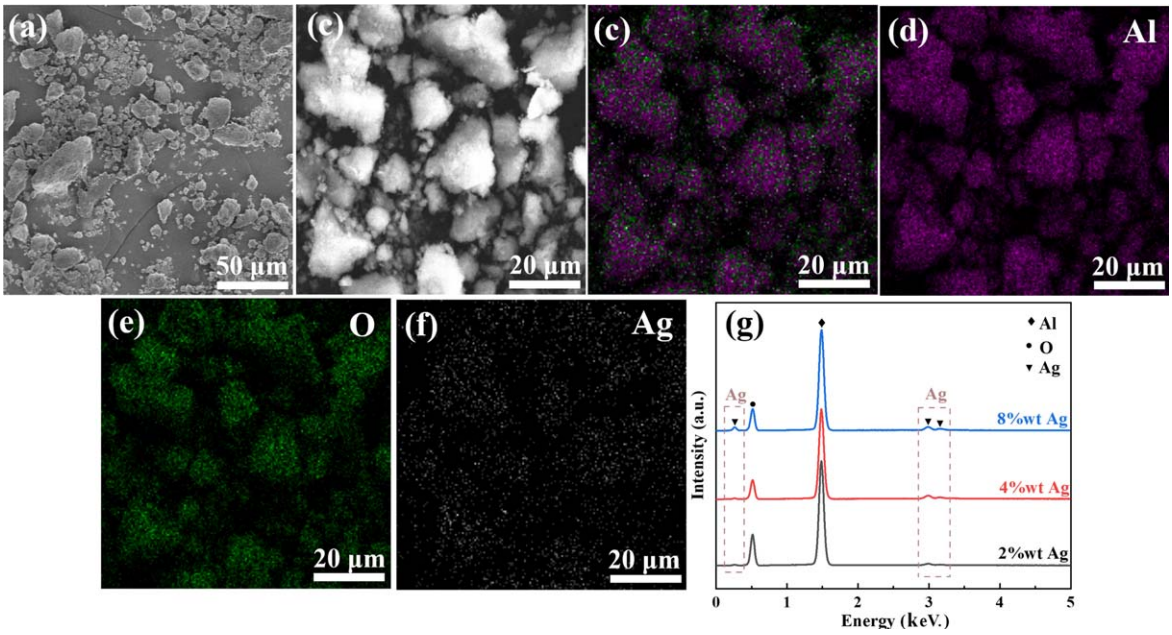

Figure 3. (a), (b) Representative SEM images of the Ag/nano-γ-Al_2O_3 catalysts (8 wt% Ag). (c) Overall element mapping. (d) Al, (e) O and (f) Ag elements. (g) EDX spectra of the Ag/nano-γ-Al_2O_3 catalysts with different Ag contents.

during the synthesis process is shown in figure S2. One can see a series of peaks in the wavelength range of 700–900 nm, which are assigned to atomic Ar transitions between excited 4p–4s states [28]. Intensive peaks ranging from 300 to 400 nm are also observed. They are indexed to the second positive system (SPS) of nitrogen [29]. Nitrogen-related features are reasonably attributed to the ambient air outgassed from the porous structure of the treated substrate powder, which are very sensitive to detection by OES analysis. There is a noticeable band at 285–300 nm, which is ascribed to the OH band. This suggests the dissociation of water molecules in plasma. The characteristic peak of silver should be at 350 nm but it was not observed in the spectrum, perhaps due to the low resolution of the instrument and interference with nitrogen bands. In addition, the inset, in figure S2 in the supplementary material, shows a photograph of the plasma discharges during the experiment, where numerous filaments with purple color are visualized.

SEM images of Ag/nano-γ-Al_2O_3 (8 wt% Ag) reveal that the catalysts have flake-like morphology and are randomly scattered in the field of view (figure 3(a)). A close examination of the surface suggests the presence of ultrasmall particles (figure 3(b)), which were first suspected to be AgNPs. To confirm the above results, EDX characterization of the same image area was provided. Elemental mapping results show the existence of Ag (white), Al (purple) and O (green) signals, where Ag fits well with the particle domains (figures 3(c)–(f)). This indicates the formation of silver particles on the γ-Al_2O_3 support. The EDX spectra of catalysts with diverse Ag contents further confirm the presence of Ag, Al and O signals, in which the intensity of the Ag signal gradually increases with the Ag loading content (figure 3(g)).

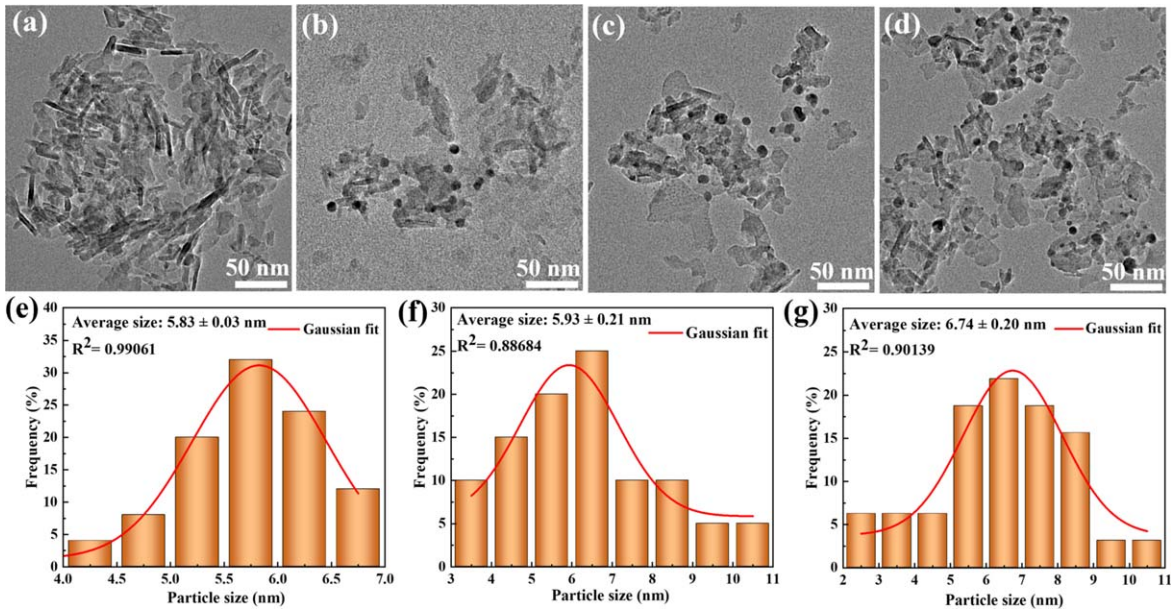

Figure 4. (a)–(d) TEM images of the Ag/nano-γ-Al_2O_3 with different Ag contents: (a) 0 wt%, (b) 2 wt%, (c) 4 wt%, and (d) 8 wt%. (e)–(g) The corresponding size distribution histograms of the AgNPs.

Thus, the Ag content of the catalysts can be controlled by tuning the processing parameters.

Figures 4(a)–(d) show TEM images of the bare nano-γ-Al_2O_3 support as well as the Ag/nano-γ-Al_2O_3 catalysts with various Ag contents (2 wt%, 4 wt% and 8 wt%). From the bare nano-γ-Al_2O_3, an overlapping irregular arrangement of rod and sheet alumina nanostructures can be observed (figure 4(a)). TEM images of the Ag/nano-γ-Al_2O_3 samples clearly show the existence of AgNPs (black dots) on the γ-Al_2O_3 surfaces, and the number of particles appears to grow with the increase in the silver nitrate concentration in the solution. In addition, these AgNPs are not aggregated together, even when prepared at 8 wt% concentration of $AgNO_3$. This indicates that the AgNPs are well dispersed on the γ-Al_2O_3. Size distribution histograms of the AgNPs were also created by measuring 200 randomly selected particles from the TEM images. It was found that the AgNPs have rather narrow size distributions from 2 to 11 nm, with a mean diameter of 5.83 nm, 5.93 nm and 6.74 nm for the 2 wt%, 4 wt% and 8 wt% Ag/nano-γ-Al_2O_3 catalysts, respectively (figures 4(e)–(g)).

It is well recognized that the difference in the electron densities of diverse elements would lead to distinguishable bright and dark areas in the same high-resolution TEM (HRTEM) imaging field [30]. Thus, in our study, HRTEM characterization was performed for 8 wt% Ag/nano-γ-Al_2O_3 to gain a better insight into the particles. Mass–thickness contrast can be readily visualized in the image, inferring the formation of the AgNPs on the γ-Al_2O_3 (figure 5(a)). Lattice fringes can also be clearly discerned within the particles. By measuring the distance across parallel atomic planes in two typical particles, the *d*-spacing is estimated to be 0.229 nm (figure 5(b)) and 0.197 nm (figure 5(d)), matching well with the (111) and (200) planes of the AgNPs. The corresponding fast Fourier transform (FFT) patterns further suggest that the plasma-generated AgNPs possess good crystallinity. Therefore, DBD plasma proves to be capable of converting silver ions into metallic species without chemical reductants.

Figure 6 shows the XRD patterns of Ag/nano-γ-Al_2O_3 with different Ag contents (0 wt%–8 wt%). All spectra consist of the characteristic peaks of the γ-Al_2O_3 phase at 19.45°, 31.94°, 37.60°, 39.49°, 45.86°, 60.90°, 67.03° and 85.02°, relating to the (111), (220), (311), (222), (400), (511), (440) and (444) planes (JCPDS #10-0425), respectively [31]. However, the spectral feature of AgNPs has not been detected in the 1 wt%–4 wt% Ag/nano-γ-Al_2O_3 samples. This might be due to the rather low content of AgNPs in the catalysts or because the generated AgNPs have good dispersion and ultrasmall particle size. For the 8 wt% Ag/nano-γ-Al_2O_3, the spectrum displays apparent diffraction peaks of Ag at 38.2°, 44.4°, 64.6°, 77.6° and 81.8°, which are indexed, respectively, to the (111), (200), (220), (311) and (222) planes (JCPDS #87-0720) [32]. The increase in the Ag content in the products with respect to the precursor concentration is also reflected by the color of the sample. For pure γ-Al_2O_3 or Ag/nano-γ-Al_2O_3 with a Ag content below 2 wt%, the products are completely white, but become slightly brown and eventually gray once the Ag content reaches 4 wt% and 8 wt% (figure S3).

XPS analysis was further used to examine the chemical composition and binding information for the prepared Ag/nano-γ-Al_2O_3. The overall XPS spectrum given in figure 7(a) shows the existence of Ag, Al, C and O elements, as indicated by the peaks relating to Ag 3d (371 eV), Al 2s (120 eV), Al 2p (74.5 eV), C 1s (284 eV) and O 1s (531 eV). Deconvolution of the Ag 3d band reveals the presence of two bands at ~368 eV and ~374 eV, with an energy gap of 6.0 eV (figure 7(b)). This band gap is characteristic of the oxidation state of silver in the $3d_{5/2}$–$3d_{3/2}$ spin–orbit split transition. The Ag $3d_{5/2}$ spectrum was further fitted using the

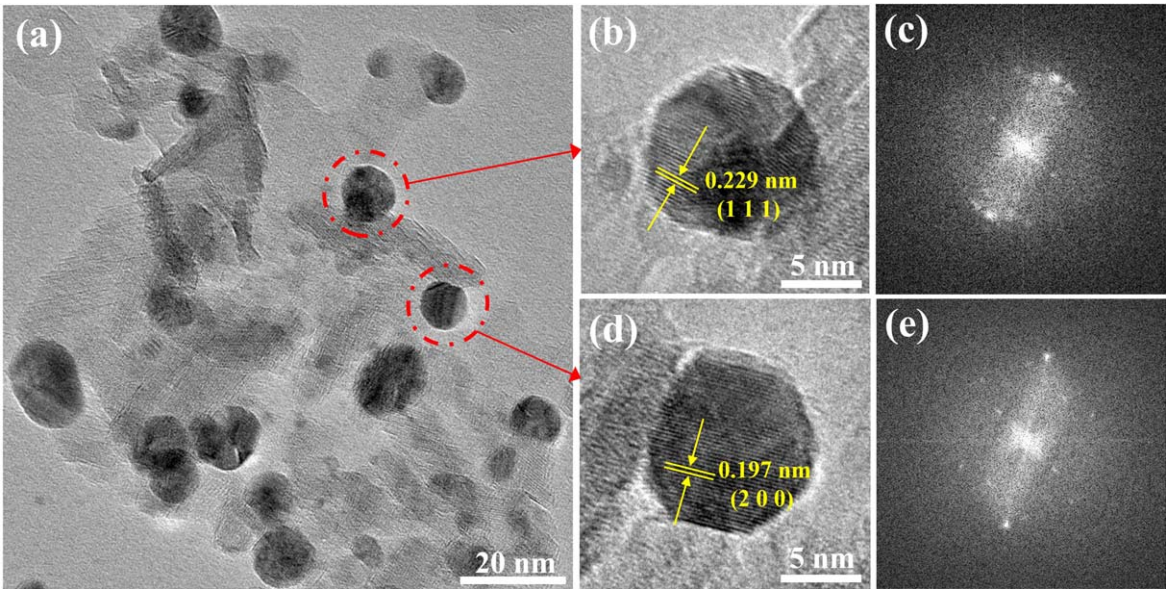

Figure 5. (a) TEM image of 8 wt% Ag/nano-γ-Al_2O_3. (b) HRTEM image of a salient Ag particle showing the (111) crystal plane and (c) the corresponding FFT pattern. (d) HRTEM image of a Ag particle showing the (200) crystal plane and (e) the related FFT pattern.

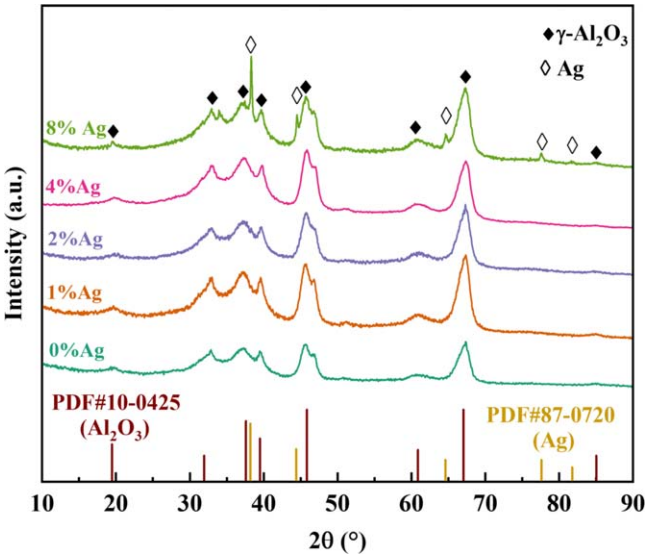

Figure 6. XRD patterns of Ag/nano-γ-Al_2O_3 with different Ag contents.

Gaussian–Lorentzian function to gain better insight into the binding information. One can see two sub-bands at 368.5 eV and 367.7 eV, corresponding to the metallic state (Ag^0) and the oxidation state (Ag^+) of silver. In general, the binding energy of metallic Ag $3d_{5/2}$ is 367.9 eV, while in our case the peak shifts obviously to a higher binding energy. This was attributed to the different charging effect induced by the interaction between Ag and γ-Al_2O_3 [33]. The valence state of Ag species was confirmed by the DRUV analysis, where absorption bands of the silver cations (Ag^+, 206 nm) and Ag^0 (288 nm, 350 nm) were observed in samples with various Ag contents (figure S4). Deconvolution of the Al 2p band reveals the presence of two bands at 73.80 eV and 74.56 eV, representing Al_2O_3 and $Al(OH)_3$, respectively (figure 7(c)). The O 1s spectrum consists of three components at 530.24 eV, 531.24 eV and 532.08 eV (figure 7(d)), relating to oxygen in three environments: surface oxygen with silver (Ag–O, 530.24 eV), oxygen in alumina (Al_2O_3, 531.24 eV) and adsorbed oxygen (e.g. H_2O).

3.2. Catalytic evaluation of the Ag/Al_2O_3 via CO oxidation reactions

We have demonstrated the preparation of Ag/γ-Al_2O_3 catalysts by the DBD plasma technique. Table S1 shows the synthesis of catalysts using the plasma method, indicating a high degree of flexibility in the plasma configurations. To evaluate their catalytic performance, Ag/γ-Al_2O_3 was applied in CO oxidation reactions. Figure 8 demonstrates the normalized CO conversion rate versus temperature during the temperature programmed reaction. The catalytic curves of 0.5 wt% and 1 wt% Ag/nano-γ-Al_2O_3 display the same trend, in which the CO conversion increases gradually with the rise of the procedure temperature, until conversions of 92.7%, and 96.0% were achieved at 700 °C. In the reaction process for 2 wt%, 4 wt% and 8 wt% Ag/nano-γ-Al_2O_3, the CO conversion rate increases stepwise with increase in temperature, reaching 100% conversion at 300 °C. Once the temperature is above 300 °C, the CO conversion efficiency remains constant at 100%, indicating that these three catalyst recipes have higher catalytic activity and lower onset temperature for CO oxidation. Besides, for the catalysts with 4 wt% or lower Ag content, CO oxidation is almost negligible at 100 °C, but reaches 20% when using 8 wt% Ag/nano-γ-Al_2O_3 at the same temperature. In view of this, a control experiment was performed under the same temperature program using a bare nanosized γ-Al_2O_3 support. The results show that the CO conversion efficiency gradually improves with increase in temperature, reaching the maximum conversion rate of 79.7%

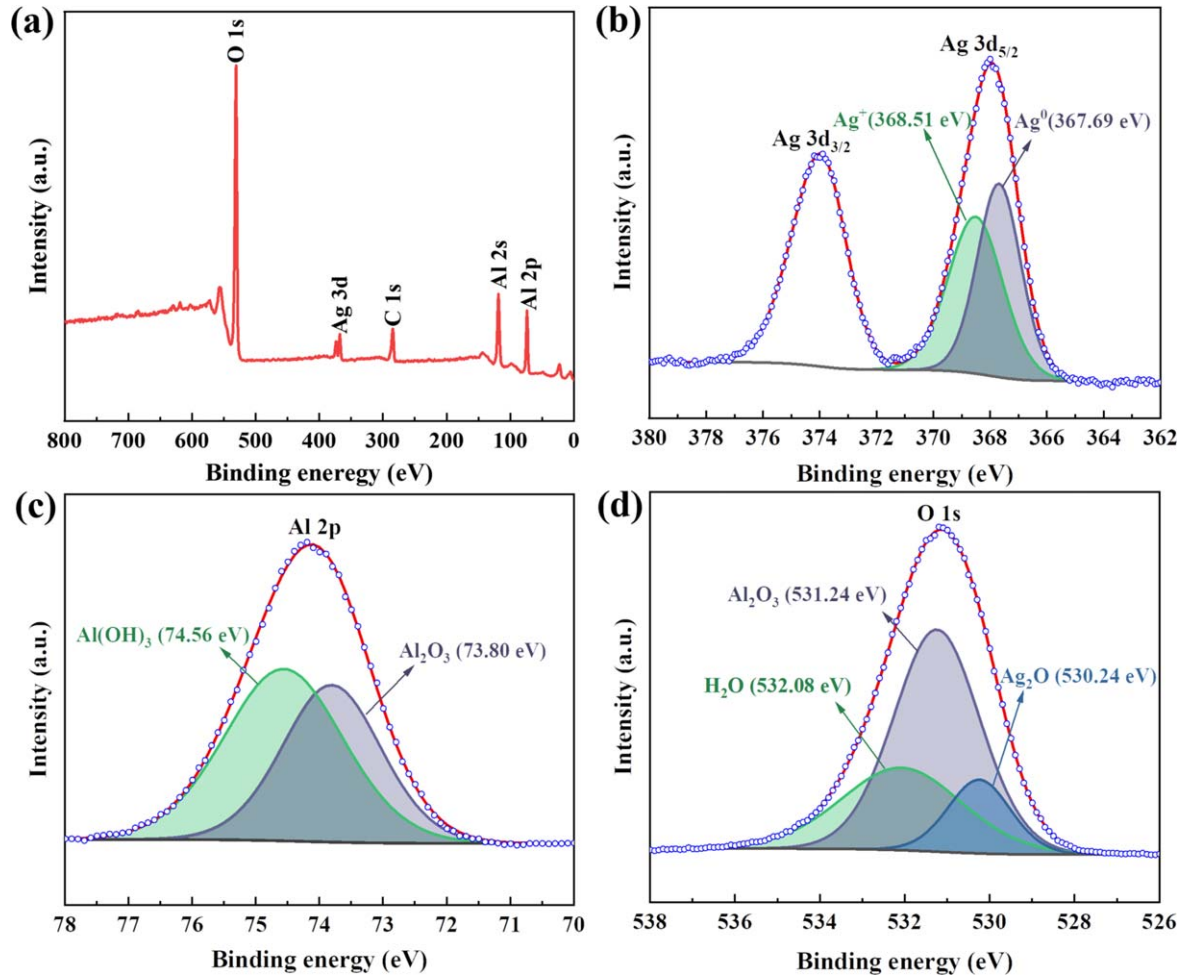

Figure 7. (a) Overall XPS spectrum of the plasma-prepared Ag/nano-γ-Al_2O_3. (b)–(d) High-resolution XPS spectrum of (b) Ag 3d, (c) Al 2p and (d) O 1s.

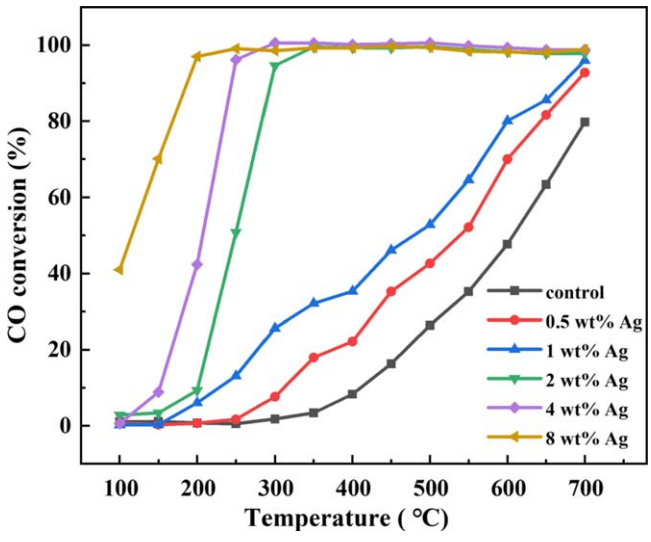

Figure 8. CO oxidation on the DBD plasma-generated Ag/nano-γ-Al_2O_3 catalysts with different Ag contents.

at 700 °C. This reveals the remarkably improved catalytic activity with increase in the Ag content.

Catalyst stability was evaluated by resetting the TPSR program and conducting four consecutive CO catalytic experiments using 8 wt% Ag/nano-γ-Al_2O_3. One can see that the catalytic curves of the four cycles are similar, and the catalytic effect of the first temperature increase is slightly lower than that of the rest (figure S5). The possible reason is that high temperature in the first catalytic cycle causes additional activation of the catalyst, resulting in the catalyst showing higher activity over the rest of the temperature increase cycle.

Apart from Ag content, the size effect of the γ-Al_2O_3 support on catalytic performance was investigated by preparing 2 wt% Ag/micro-γ-Al_2O_3 catalysts. Figure 9(a) shows a typical TEM image of 2 wt% Ag/micro-γ-Al_2O_3 catalysts obtained by the DBD plasma method. The catalyst supports exhibit an irregular plate-like morphology with numerous AgNPs deposited on the surface. The particle size is in the range of 4–12 nm, with a mean diameter of 6.95 nm (figure 9(b)). The FFT pattern shows the presence of highly symmetrical diffraction spots, revealing that the catalysts have good crystallinity (figure 9(c)). This is also confirmed by the HRTEM image, where parallel lattice fringes relating to the (111) plane were observed (figure 9(d)).

The catalytic performance given in figure 10 further suggests that Ag/nano-γ-Al_2O_3 catalysts have better activity than Ag/micro-γ-Al_2O_3, as reflected by the higher catalytic

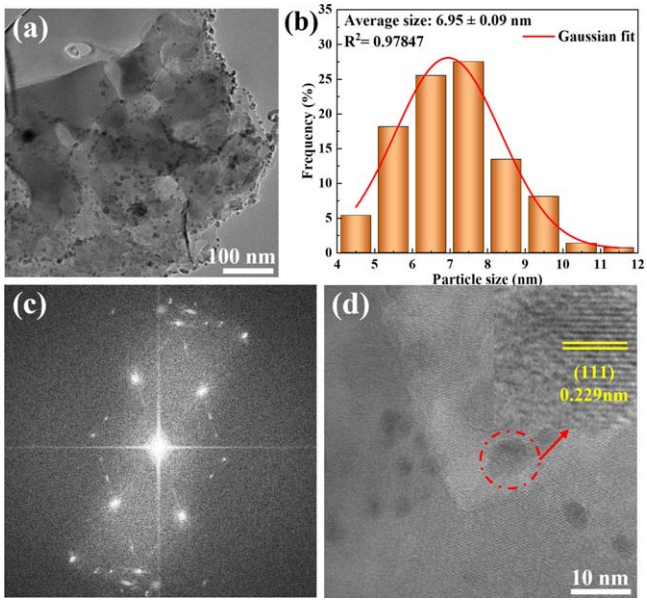

Figure 9. (a) TEM image of the plasma-generated 2 wt% Ag/micro-γ-Al_2O_3. (b) Size distribution of the AgNPs and (c) the corresponding FFT pattern. (d) A typical HRTEM image of 2 wt% Ag/micro-γ-Al_2O_3.

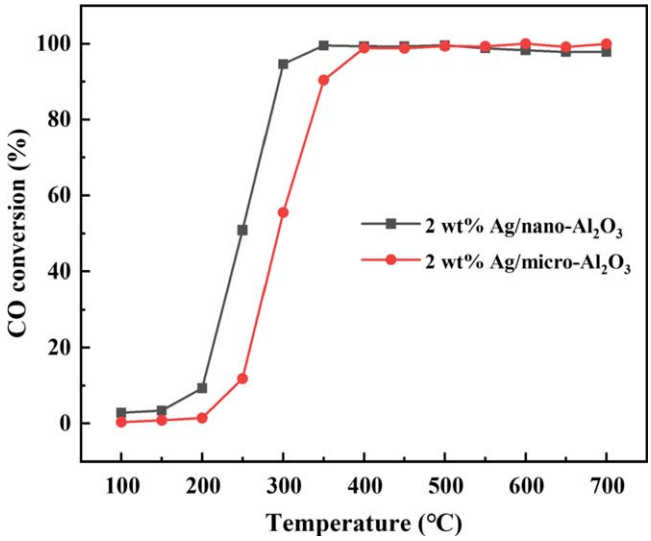

Figure 10. CO oxidation over 2 wt% Ag/micro-γ-Al_2O_3 and 2 wt% Ag/nano-γ-Al_2O_3 catalysts.

activity and lower onset temperature for CO oxidation. Although both catalysts can achieve 100% CO conversion, Ag/nano-Al_2O_3 exhibits higher catalytic performance at somewhat lower temperatures than Ag/micro-γ-Al_2O_3 catalysts. This might be due to the larger specific surface area of Ag/nano-Al_2O_3. BET analysis was performed to verify this result (table S2). For the Ag/nano-γ-Al_2O_3 catalysts, the BET surface area is measured to be 133.2 $m^2\ g^{-1}$, much larger than that of the Ag/micro-γ-Al_2O_3 catalysts (3.4 $m^2\ g^{-1}$). The direct consequence of the enhanced surface area is an increase in the interaction between gas molecules and the active sites of the catalysts, which is beneficial for CO oxidation.

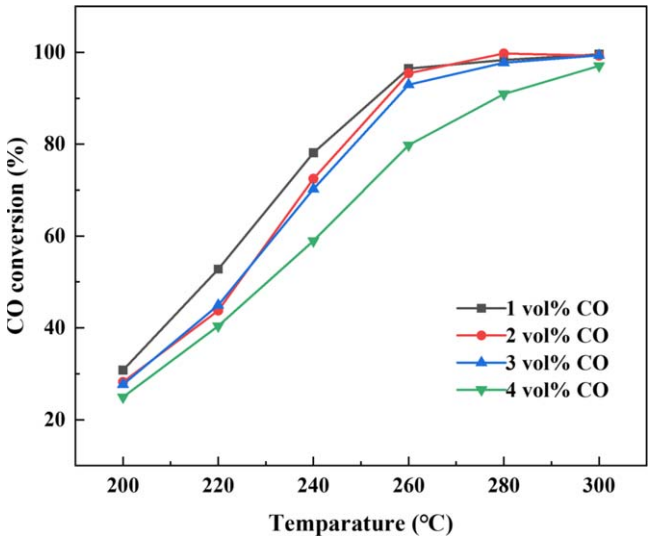

Figure 11. CO oxidation at different CO concentrations for 2 wt% Ag/nano-γ-Al_2O_3 catalysts.

The benefits of preparing catalysts using the DBD plasma method were also examined by comparison with the traditional calcination approach. We prepared 2 wt% Ag/nano-γ-Al_2O_3 catalysts following the standard calcination procedure (denoted as Ag/nano-γ-Al_2O_3-C), and evaluated their catalytic performance. Figure S6(a) shows a TEM image of 2 wt% Ag/nano-γ-Al_2O_3-C. Partially aggregated AgNPs of quasi-spherical shape are clearly seen on the surface of the Al_2O_3 support. The particle size distribution is in the range 5–12 nm, and the mean particle diameter is 8.4 nm (figure S6(b)). This is slightly larger than that of the DBD plasma-prepared catalysts. An advantage of the plasma technique is that metal particles can be charged during the synthesis process, making them repel each other to prevent agglomeration [34]. The AgNPs also possess a crystalline structure, as reflected by the HRTEM image and the FFT pattern (figures S6(c)–(e)). When applied in CO oxidation reactions, the DBD plasma-generated samples demonstrate 100% conversion of CO at a lower operational temperature, with a steeper temperature dependency than for catalysts prepared by the standard calcination approach (figure S7). This indicates that the catalytic performance of the plasma-obtained catalysts is considerably better than that of catalysts prepared by the traditional method. Such phenomena were also reported by Neyts *et al* [35], Whitehead [36], Bogaerts *et al* [37, 38] and Ostrikov *et al* [39, 40]. Table S3 provides an overview of different methods for the synthesis of Ag/γ-Al_2O_3 catalysts to better illustrate the pros and cons of the DBD plasma method.

The influence of CO concentration on CO conversion rate was explored by varying CO concentration from 1% to 4% using Ag/nano-γ-Al_2O_3 catalysts, as shown in figure 11. In all cases, the CO conversion rate increased with the rise in temperature, and 100% conversion can be achieved at 300 °C when the CO concentration is below 3%. It is also noted that a lower CO concentration contributed to a higher conversion rate at the same temperature, in agreement with the results of Camposeco and Zanella [41] and Koo *et al* [42].

4. Conclusions

In summary, we successfully prepared Ag/γ-Al_2O_3 catalysts with different Ag contents by the DBD plasma method. Using SEM, TEM, XRD, XPS and other characterization methods this approach is demonstrated to be capable of converting silver ions into metallic species through presumed reduction by plasma electrons. Results show that AgNPs with good dispersion, uniformity and crystalline nature were formed on the surface of the alumina support. The CO oxidation experiments show that the catalysts have good activity and stability in CO oxidation reactions, where the catalytic effect appears at a threshold Ag content and improves with further increase in the Ag concentration. Moreover, due to the increased specific surface area together with the enhanced interactions between gas molecules and the catalysts, the Ag/nano-γ-Al_2O_3 catalysts demonstrate higher activity than the Ag/micro-γ-Al_2O_3 catalysts with the same Ag content. We also made a comparison between standard thermal calcination and the plasma preparation method, from which the plasma-generated catalysts exhibit better catalytic performance than those prepared by the calcination method. In addition, a lower CO concentration was found to contribute to a higher conversion rate at the same temperature using Ag/nano-γ-Al_2O_3 catalysts. The present study demonstrates that supported metal catalyst can be prepared by the plasma process at low temperature in inert Ar gas without the addition of reducing agents such as hydrogen. This makes the proposed approach safe to scale up and it is applicable for temperature-sensitive supports. In conclusion, plasma technology provides a green and efficient method for catalyst preparation, and produces active ingredients with smaller particle sizes and higher dispersion than traditional methods, thus improving catalytic performance.

Acknowledgments

We would like to acknowledge financial support from National Natural Science Foundation of China (Nos. 52004102 and 22078125), Postdoctoral Science Foundation of China (No. 2021M690068), Fundamental Research Funds for the Central Universities (Nos. JUSRP221018 and JUSRP622038), Key Laboratory of Green Cleaning Technology and Detergent of Zhejiang Province (No. Q202204) and Open Project of Key Laboratory of Green Chemical Engineering Process of Ministry of Education (No. GCP202112).

References

[1] Védrine J C 2017 *Catalysts* **7** 341
[2] García-Serna J, Piñero-Hernanz R and Durán-Martín D 2022 *Catal. Today* **387** 237
[3] Witoon T *et al* 2022 *Chem. Eng. J.* **428** 131389
[4] Marek E J and García-Calvo Conde E 2021 *Chem. Eng. J.* **417** 127981
[5] Chen Y, Qian S and Feng K 2022 *Chem. Eng. Sci.* **253** 117597
[6] Wu K J, Bohan G M D V and Torrente-Murciano L 2017 *React. Chem. Eng.* **2** 116
[7] Ahmed J *et al* 2022 *Powder Technol.* **412** 117975
[8] Zhang X L *et al* 2021 *Chem. Eng. Sci.* **238** 116588
[9] Ma X T *et al* 2020 *Chem. Eng. Sci.* **220** 115648
[10] Lin L L *et al* 2021 *J. Taiwan Inst. Chem. Eng.* **122** 311
[11] Li X H *et al* 2022 *React. Chem. Eng.* **7** 346
[12] Li X H, Zhao C-X and Lin L L 2022 *Chem. Eng. Sci.* **260** 117849
[13] Lin L L *et al* 2022 *Ind. Eng. Chem. Res.* **61** 2183
[14] Lin L L *et al* 2021 *Chem. Eng. J.* **417** 129355
[15] SriBala G *et al* 2019 *J. Clean. Prod.* **209** 655
[16] Delikonstantis E *et al* 2022 *ACS Energy Lett.* **7** 1896902
[17] Rui L C *et al* 2022 *Chem. Eng. Res. Des.* **186** 125
[18] Di L B *et al* 2016 *Plasma Sci. Technol.* **18** 544
[19] Wang B W *et al* 2019 *Plasma Sci. Technol.* **21** 065503
[20] Ji H H, Lin L L and Chang K 2023 *J. CO_2 Util.* **68** 102351
[21] Liu Y *et al* 2020 *Plasma Sci. Technol.* **22** 034016
[22] Li Y *et al* 2023 *Fuel Process. Technol.* **242** 107655
[23] Xu S *et al* 2020 *ACS Catal.* **10** 12828
[24] Han S W *et al* 2016 *Chem. Eng. J.* **283** 99
[25] Zhou Y, Wang Z Y and Liu C J 2014 *Catal. Sci. Technol.* **5** 69
[26] Sun T *et al* 2022 *Ind. Eng. Chem. Res.* **61** 152
[27] Lee K *et al* 2021 *J. Ind. Eng. Chem.* **93** 461
[28] Xu H *et al* 2019 *Mater. Lett.* **255** 126532
[29] Lin L L *et al* 2019 *React. Chem. Eng.* **4** 891
[30] Wang J L, Ando R A and Camargo P H C 2014 *ACS Catal.* **4** 3815
[31] Ma C *et al* 2019 *Ind. Eng. Chem. Res.* **58** 1848
[32] Wang F *et al* 2019 *ACS Catal.* **9** 1437
[33] Jing X *et al* 2014 *RSC Adv.* **4** 27597
[34] Lin L L and Wang Q 2015 *Plasma Chem. Plasma P.* **35** 925
[35] Neyts E C *et al* 2015 *Chem. Rev.* **115** 13408
[36] Whitehead J C 2019 *Front. Chem. Sci. Eng.* **13** 264
[37] Bogaerts A *et al* 2020 *Phys. D: Appl. Phys.* **53** 443001
[38] Girard-Sahun F *et al* 2022 *Chem. Eng. J.* **442** 136268
[39] Weltmann K-D *et al* 2019 *Plasma Process Polym.* **16** 1800118
[40] Ma S *et al* 2022 *Chem. Eng. J.* **435** 134859
[41] Camposeco R and Zanella R 2022 *Environ. Sci. Pollut. Res.* **29** 76992
[42] Koo K Y, Jung U H and Yoon W L 2014 *Int. J. Hydrogen Energ.* **39** 5696